
EvoScene-VLA: Evolving Scene Beliefs Inside the Action Decoder for Chunked Robot Control

Chushan Zhang¹ Ruihan Lu² Jinguang Tong¹ Xuesong Li¹ Yikai Wang³ Hongdong Li¹

¹Australian National University ²The University of Queensland ³Beijing Normal University

Abstract

Chunked vision-language-action (VLA) policies predict multi-step robot controls, conditioning each update on the current visual observation alone. Yet robot actions cause contact, occlusion, and object motion, and the geometry that later decisions depend on can change before the next visual update arrives. Spatial VLAs improve current-frame geometry. Temporal VLAs aggregate past frames. Neither maintains an action-updated scene prior across chunks. We argue for a persistent action-updated scene state across control calls, and introduce EvoScene-VLA. Its recurrent scene prefix carries a geometry-aware scene state across chunks. At each vision-language model (VLM) call, the VLM combines scene information from the current observation with the action-updated prior from the previous chunk; the action decoder outputs both the next action chunk and a compact scene update. This update becomes the next prior, which the VLM corrects against the new observation when the next call arrives. Each control call therefore starts from a scene prior that reflects both recent actions and fresh visual evidence. During training, **Scene Predictor** supplies future scene-token targets, and **Geometric Anchor** aligns scene slots with frozen depth and 3D teachers. We discard both modules at deployment. On 31 RoboTwin tasks, EvoScene-VLA raises average success from 87.2% to 89.1% in fixed evaluation and from 86.1% to 88.5% in randomized evaluation. On the Galaxea R1-Lite real robot, EvoScene-VLA outperforms all baselines.

1 Introduction

Chunked vision-language-action policies predict multi-step robot controls, but they usually condition scene context on observations rather than on the robot’s own actions. Yet actions can change the scene before the next observation arrives: wiping the counter changes the surface state, closing a drawer hides its contents, and lifting a cup leaves the shelf slot below it empty. Within a chunk, the visual context may not reflect such changes at all. Across chunks, fresh observations do arrive, but the policy still lacks a compact record of how its recent actions transformed the scene, and must re-infer those changes from partial, noisy, or occluded visual evidence.

Spatial VLAs [28, 19, 17, 18, 46] improve geometric reasoning within a single image through depth supervision, 3D encoding, or multi-view features. These methods help when the full scene is visible, but they reason from current observations alone and do not update scene geometry once actions have changed it. Temporal VLAs [30, 15, 20, 6, 44] retain past observations through memory banks, trace prompts, or recurrent states, yet past observations alone do not specify how recent or planned actions should update the scene. Action-conditioned prediction methods [45, 43] anticipate future representations, but consume each prediction inside the current decision and discard it afterwards. The missing piece, we argue, is an action-updated scene representation. The policy should pass this representation to the next control call as a prior.

A useful scene representation for chunked control needs three properties. It should persist across chunks, so the policy is not forced to re-infer it from each new observation. It should update under the actions the policy generates, since those actions change the scene. And it should correct against

Task	Initial Scene	LingBot-VLA*			EvoScene-VLA (Ours)		
		Start	Middle	End	Start	Middle	End
Open Microwave							
Stack Three Blocks							
Put Object Cabinet							

changed / ambiguous region
 LingBot-VLA next action
 EvoScene-VLA next action
 action-scene mismatch
 recovered

Figure 1: **Qualitative analysis of chunked-control failures.** During one action chunk, the scene can drift from the planning observation, so an action-only baseline commits to a stale target. In three RoboTwin tasks (microwave handle, block stacking, cabinet placement), the baseline follows this stale target and stalls mid-chunk (×). EvoScene-VLA carries an action-updated scene prior into the chunk, so each predicted action uses the scene state for its own step and completes the rollout (✓).

each new observation, so prediction errors do not accumulate. Missing any one of these undermines the design: no persistence means no cross-chunk context, no action update means no post-action prior, and no correction means errors compound.

We propose EvoScene-VLA, which implements this action-updated scene prior as a recurrent scene prefix. The prefix contains two groups of scene tokens at each step: one read from the current observation, and one inherited from the previous chunk. At each vision-language model call, the model refines both groups against the new image. The action decoder then co-denoises the action chunk and a matched scene chunk in a single flow-matching pass. After denoising, the resulting scene chunk becomes the inherited group in the next chunk’s prefix. The deployed model therefore carries an action-updated prior into each new chunk without any separate online module for memory, prediction, or correction.

The action decoder needs supervision for the co-denoised scene chunk, but the deployed model should not depend on an auxiliary predictor. Prefix scene tokens also need geometric grounding, or they risk encoding generic appearance. We address both issues with two training-only modules: a **Geometric Anchor** that grounds scene tokens in 3D, and a **Scene Predictor** that supplies future-frame targets. Geometric Anchor operates at two levels: a *local* depth anchor [29] aligns each scene token with per-pixel depth, while a *global* 3D-foundation-model (3DFM) anchor [36] aligns it with scene-level features through a shared decoder that handles both current and future representations. Scene Predictor maps the current scene and action sequence to future scene representations, supervised by future-frame 3DFM features; flow matching then distills these targets into the action decoder’s scene chunk. At inference, both modules are discarded, leaving only the recurrent scene prefix and the scene chunk co-denoised by the action decoder.

On 31 RoboTwin tasks [25], EvoScene-VLA raises the average success rate from 87.2% to 89.1% under fixed evaluation and from 86.1% to 88.5% under randomized initial conditions. The gain is in fact larger under randomized conditions than under fixed ones, suggesting the scene prior is robust to pose and layout variation. Closed-loop trials on a Galaxea R1-Lite [12] dual-arm platform confirm similar gains under real-world deployment. Ablations further show cumulative contributions from future-scene supervision with the global anchor, local depth anchoring, and the recurrent prior.

Our contributions are threefold.

- We show that an action expert can produce an action-updated scene prior for the next control call. It uses a recurrent scene prefix and action–scene co-denoising, without an auxiliary online predictor at inference.

- We introduce a two-level *Geometric Anchor* that combines local depth supervision with a global 3D-foundation-model anchor, sharing one decoder to ground both current and future scene latents.
- We report consistent gains on the RoboTwin benchmark and on a Galaxea R1-Lite real-robot platform, with ablations showing cumulative contributions from future-scene supervision, geometric anchoring, and the recurrent prior.

2 Related Work

VLA policies use VLM backbones to map images and language instructions to chunked motor controls. RT-2 [3], π_0 [1], and OpenVLA [13] establish this paradigm. EvoScene-VLA adds a recurrent scene prefix to the chunked decoder. We review geometric, temporal, and flow-based foundations for this design.

Geometric scene representation. Spatial VLAs add geometry to the VLM prefix or visual encoder. SpatialVLA [28] projects 3D-aware features into a spatial token grid, QDepth-VLA [19] supervises quantized depth tokens, Spatial Forcing [17] enforces geometric consistency, and 3DS-VLA [18] and VLA-4D [46] add multi-view or temporal 3D features. A parallel line uses 3D scene state for manipulation: PerAct [31], RVT [8, 9], 3D Diffusion Policy [42], and ManiGaussian [24]. Persistent reconstruction systems such as DUST3R [35], MAST3R [16], and CUT3R [34] maintain state tokens for dense 3D reconstruction. These methods improve current or observation-driven geometry. They do not advance a policy-facing scene prior with the robot’s own action chunk. EvoScene-VLA updates a compact geometric prior along the generated action sequence, so the next VLM call can correct an already-advanced scene state.

Temporal memory and action-conditioned prediction. Temporal VLAs retain observed history across control calls. MemoryVLA [30] maintains a summary-token memory, HAMLET [15] and HiF-VLA [20] use history-aware attention, Embodied-SlotSSM [6] applies slot state-space models, TraceVLA [44] prompts the VLM with visual traces, and AVA-VLA [41] aligns action and visual history. Related approaches learn trajectory representations from video [37, 11] or transfer across heterogeneous demonstrations [33]. Other methods predict future state from actions. FLARE [45] inserts learnable future tokens into the VLM, UP-VLA [43] uses action-conditioned image or feature prediction, world models [39, 10, 38, 4] roll out latent futures, and video-prediction policies [7, 2, 14] generate or condition on pixel-level futures. These methods record observed history or predict a future for the current decision. They do not keep a self-correcting prior across chunk boundaries. EvoScene-VLA persists an action-updated scene prior through the recurrent scene prefix and corrects it with the next observation.

Flow matching and diffusion policies. Flow-matching and diffusion policies model robot control as trajectory denoising. Diffusion Policy [5] popularized diffusion-based continuous control. π_0 [1], RDT [22], Octo [26], and flow-matching VLAs [21, 23] scale this formulation to pretrained VLAs. Consistency Policy [27] accelerates sampling. These methods denoise actions only, so their decoders do not evolve scene state. EvoScene-VLA co-denoises the action chunk and the evolved scene representation in one flow-matching pass. This joint denoising grounds each action in the recurrent scene prior without adding an inference-time predictor.

3 Method

3.1 Overview

EvoScene-VLA extends LingBot-VLA [40] with a recurrent scene prefix for chunked control. As shown in Fig. 2, we add two slot groups to the VLM prefix: *observation slots* that gather evidence from the current image, and *prior slots* that inherit the scene state denoised by the action expert in the previous chunk. The action expert then co-denoises the next action chunk together with a matched scene chunk in a single flow-matching pass, and the denoised scene token at the executed step is fed back as the prior for the next call. Two training-only modules supervise this loop: **Geometric Anchor** (Sec. 3.3) grounds scene slots in metric geometry, and **Scene Predictor** (Sec. 3.4) supplies

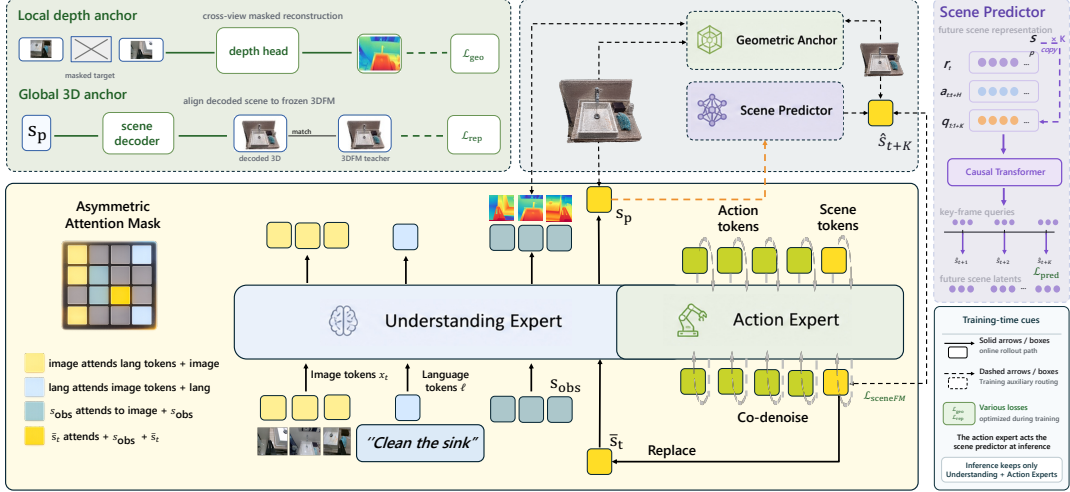


Figure 2: **Pipeline Overview.** The policy receives multi-view images, an instruction, and the robot state. The VLM prefix contains image and language tokens, per-view observation slots, and recurrent prior slots. An asymmetric attention mask lets observation slots read the current views and lets prior slots absorb this evidence while preserving the pretrained image and language pathways. During training, Geometric Anchor grounds the scene slots with Monocular Depth Teacher and 3D-foundation-model features, and Scene Predictor supplies future scene-token targets to train the action expert. At inference, the action expert denoises the actions and matched scene tokens together in the flow-matching sampling. The scene token at the executed step becomes the prior for the next VLM call, so each action chunk starts from an action-updated, observation-corrected scene prior.

future scene-token targets. At inference, EvoScene-VLA discards both training-only modules and retains only the recurrent scene prefix and action–scene co-denoising.

3.2 Recurrent Scene Prefix

Let D denote the VLM hidden dimension, V the fixed camera views (head, left wrist, right wrist), and N the number of slots in each observation or prior group. EvoScene-VLA augments the VLM prefix with two groups of scene slots: per-view *observation slots* $s_{\text{obs}}^{(v)} \in \mathbb{R}^{N \times D}$, $v \in \{1, \dots, V\}$, which gather geometric evidence from each camera, and a single set of *prior slots* $\bar{s}_t \in \mathbb{R}^{N \times D}$, which inherit the action-updated scene state from the previous chunk. Together with the multi-view image input x_t and language instruction ℓ , the prefix is ordered:

$$[x_t, s_{\text{obs}}^{(1:V)}, \bar{s}_t, \ell]. \quad (1)$$

At the first chunk, \bar{s}_t is initialized from learnable scene embeddings; for later chunks, it carries the recurrent state denoised by the action expert at the previous step (Sec. 3.5). The VLM thus consumes a prior when one exists and falls back to learned embeddings otherwise.

An asymmetric attention mask routes information through this prefix as illustrated in Fig. 2. Image and language tokens ignore scene slots, preserving pretrained visual and linguistic paths. Each observation slot attends to its own view’s image tokens and to other slots in its own observation group. Prior slots attend to all observation slots and to themselves, but not to image or language tokens, and no other token attends back to them. Current image evidence therefore reaches the prior slots only through the observation slots. This isolation preserves the pretrained image–language pathway intact while giving the scene state a dedicated bottleneck: only observation slots feed into the prior, and the prior never leaks back into image or language tokens. Let $s_p \in \mathbb{R}^{N \times D}$ denote the VLM output at the prior-slot positions, which we take as the corrected scene representation for the current chunk:

$$s_p = \text{VLM}_{\text{scene}}(x_t, \ell, s_{\text{obs}}^{(1:V)}, \bar{s}_t)_{\text{prior}}. \quad (2)$$

The representation s_p thus serves as a recurrent scene state. The prefix defines *where* this state lives in the architecture, but not *what* it should encode; the next two modules supply that content by

grounding the representation in geometry and training the action expert to write the next recurrent state.

3.3 Two-Level Geometric Anchor

The recurrent prefix specifies where the scene state lives but not what it should encode; without targeted supervision, the slots are free to absorb generic image features rather than 3D structure. Geometric Anchor addresses this gap with two complementary training-only branches. One branch, called **Local Anchor**, supervises each observation slot $s_{\text{obs}}^{(v)}$ through cross-view masked depth reconstruction. The other branch, called **Global Anchor**, distills a frozen 3D foundation model into the aggregated representation s_p .

3.3.1 Local Anchor: Cross-View Masked Depth Reconstruction

The local branch grounds each observation slot in per-view geometry while forcing it to integrate evidence from the other views, so that no slot can rely on its own image tokens alone. To do so, we mask one view at a time and require the head to recover its depth representation from the remaining views and the cross-view representation s_p .

Concretely, observation slots are pooled from a 256-token query bank q_{tmpl} , which we also use as the query set for a lightweight cross-attention head g_{depth} . For each target view $i \in \{1, \dots, V\}$, we mask its VLM image tokens h_{t,v_i}^{img} by broadcasting a learned embedding $m \in \mathbb{R}^D$ and pass the masked multi-view tokens together with s_p to g_{depth} :

$$\hat{f}_{t,i}^d = g_{\text{depth}}\left(q_{\text{tmpl}}, [\tilde{h}_{t,v_1}^{\text{img},(i)}, \dots, \tilde{h}_{t,v_V}^{\text{img},(i)}, s_p]\right), \quad \tilde{h}_{t,v_j}^{\text{img},(i)} = \begin{cases} m, & j = i, \\ h_{t,v_j}^{\text{img}}, & j \neq i. \end{cases} \quad (3)$$

Masking the target view removes the shortcut of copying its own VLM features, forcing g_{depth} to aggregate cross-view evidence from the unmasked tokens and from s_p . We supervise each prediction with a frozen Monocular Depth Teacher (MDT) [32] applied to the unmasked target image:

$$\mathcal{L}_{\text{geo}} = \frac{1}{V} \sum_{i=1}^V \text{SmoothL1}\left(\hat{f}_{t,i}^d, f_{t,i}^d\right), \quad f_{t,i}^d = \text{MDT}(x_{t,v_i}). \quad (4)$$

The cross-view masking loss trains observation slots and prior positions together: each $s_{\text{obs}}^{(v)}$ summarizes view-level depth, and s_p encodes geometry across views.

3.3.2 Global Anchor: 3D Foundation Model Decoding

The global branch grounds the cross-view representation s_p in metric 3D by distilling a frozen multi-view 3DFM [36]. A lightweight view-conditioned decoder g_{3D} takes a set of learnable queries q_{dec} and uses s_p from Eq. (2) as keys and values; a linear projector W_{proj} then maps the decoder output to the foundation-model feature space:

$$H_t = g_{3D}(q_{\text{dec}}; s_p), \quad P_t = W_{\text{proj}} H_t. \quad (5)$$

We supervise P_t to match the frozen foundation model’s features on the same multi-view input via an ℓ_1 loss:

$$\mathcal{L}_{\text{rep}} = \frac{1}{V} \sum_{v=1}^V \|P_t^{(v)} - Z_t^{(v)}\|_1, \quad Z_t = 3DFM(x_t). \quad (6)$$

The ℓ_1 objective regresses the foundation-model features element-wise, providing dense token-level supervision that is robust to outliers and preserves both direction and magnitude of the target representation.

3.4 Scene Predictor

Scene Predictor produces the future scene-token targets that the action expert later distills into its scene branch. Let H denote the final action offset of the action chunk. Conditioned on the current scene representation s_p and the action sequence $a_{t:t+H}$, it predicts a sequence of absolute future

scene latents at sparse key-frame steps, supervised against features from the 3D foundation model on the corresponding future frames.

The module is a causal Transformer that takes as input the robot state r_t , the current scene representation s_p , the action sequence $a_{t:t+H}$, and K key-frame query groups initialized from s_p :

$$[r_t, s_p, a_t, \dots, a_{t+H}, q_1, \dots, q_K], \quad q_i = \text{copy}(s_p), \quad i = 1, \dots, K. \quad (7)$$

Under a causal mask, each query group q_i attends to r_t, s_p , the action prefix $a_{t:t+k_i}$ up to its target step, and earlier query groups, so that the prediction at step $t + k_i$ is conditioned only on actions executed up to that step. The output is a sequence of *absolute* future scene latents $\hat{s}_{t+k_1:t+k_K}$ at sparse key-frame steps $\{k_1, \dots, k_K\} \subseteq \{1, \dots, H\}$, with each $\hat{s}_{t+k_i} \in \mathbb{R}^{N \times D}$.

Scene Predictor reuses the view-conditioned decoder (g_{3D}, W_{proj}) from Eq. (5): the same operator that grounds s_p , also decodes each predicted future latent and matches it to foundation-model features on the corresponding future multi-view frame. Let $Z_{t+k_i} = \text{3DFM}(x_{t+k_i})$ denote the future-frame teacher features:

$$\mathcal{L}_{\text{pred}} = \frac{1}{K \cdot V} \sum_{i=1}^K \sum_{v=1}^V \|\tilde{P}_{t+k_i}^{(v)} - Z_{t+k_i}^{(v)}\|_1, \quad \tilde{P}_{t+k_i} = W_{\text{proj}}(g_{3D}(q_{\text{dec}}; \hat{s}_{t+k_i})). \quad (8)$$

3.5 Joint Action–Scene Denoising

The action expert learns to denoise actions and future scene latents jointly under a single flow-matching vector field. During training, this couples motor and scene targets on a shared denoising schedule. At inference, the same denoising loop produces both the action chunk and the next recurrent prior, replacing Scene Predictor and closing the recurrence loop without any auxiliary online module.

Given the Scene Predictor outputs $\hat{s}_{t+k_1:t+k_K}$, we stack them into future-scene targets $z_0 \in \mathbb{R}^{K \times N \times D}$. We then sample a single flow-matching time $\tau \in [0, 1]$ shared between the action and scene paths, draw independent Gaussian noises ϵ_a and ϵ_s , and form straight-line interpolants

$$a_{t:t+H}^\tau = \tau \epsilon_a + (1 - \tau) a_{t:t+H}, \quad z^\tau = \tau \tilde{\epsilon}_s + (1 - \tau) z_0, \quad \tilde{\epsilon}_s := \sigma \epsilon_s, \quad (9)$$

where σ rescales the scene noise to match the empirical magnitude of z_0 , which differs from that of the action targets. The action expert receives the suffix

$$[r_t \mid z^\tau \mid a_{t:t+H}^\tau] \quad (10)$$

Under a causal suffix mask, the action expert attends to the VLM prefix cache that contains image, language, observation, and prior slots. It predicts a per-token velocity v_θ for each action and scene block. We stop gradients through both targets, so velocity matching uses

$$\mathcal{L}_{\text{sceneFM}} = \|v_\theta^{(s)}(z^\tau, \tau) - (\tilde{\epsilon}_s - z_0)\|_2^2, \quad \mathcal{L}_{\text{actFM}} = \|v_\theta^{(a)}(a^\tau, \tau) - (\epsilon_a - a_{t:t+H})\|_2^2. \quad (11)$$

$\mathcal{L}_{\text{actFM}}$ is the standard $\pi_{0.5}$ action FM loss. $\mathcal{L}_{\text{sceneFM}}$ distills future scene representations into the action expert. The action expert then serves as the inference-time scene updater. At deployment, each chunk runs one VLM forward followed by one Euler-step denoising pass; the robot executes the resulting action chunk, and the scene token at the final key-frame offset k_K becomes the prior \bar{s}_{t+1} for the next chunk. The VLM call at the next chunk corrects this prior against the new observation, closing the recurrent loop.

3.6 Training Objective

The full training objective combines the action flow-matching loss with the four scene-grounding and scene-transfer terms introduced above:

$$\mathcal{L} = \mathcal{L}_{\text{actFM}} + \lambda_1 \mathcal{L}_{\text{geo}} + \lambda_2 \mathcal{L}_{\text{rep}} + \lambda_3 \mathcal{L}_{\text{pred}} + \lambda_4 \mathcal{L}_{\text{sceneFM}}. \quad (12)$$

The four scene-side losses play three roles: \mathcal{L}_{geo} and \mathcal{L}_{rep} ground current scene representations in geometry, $\mathcal{L}_{\text{pred}}$ trains future representations in the same coordinate, and $\mathcal{L}_{\text{sceneFM}}$ transfers those representations into the action expert. We train end-to-end in a single stage. All loss weights, the number of key frames K , and the final action offset H are reported in Appendix A.

Table 1: Success rates (%) on 31 RoboTwin tasks. C and R denote Clean and Rand evaluation settings, respectively. LingBot-VLA* denotes the depth-augmented LingBot-VLA. The 31 tasks are split across three blocks for readability.

Method	Avg.↑ (%)		Place Mouse Pad		Click Bell		Open Microwave		Place Shoe		Put Obj. Cabinet		Stack Blocks Three		Beat Block Hammer		Turn Switch		Open Laptop	
	C	R	C	R	C	R	C	R	C	R	C	R	C	R	C	R	C	R	C	R
$\pi_{0.5}$	81.2	75.9	60	39	99	66	34	77	92	93	80	79	91	76	96	93	62	54	90	96
LingBot-VLA	85.3	84.1	84	88	68	60	66	54	97	95	82	80	95	90	90	85	64	75	98	97
LingBot-VLA*	87.2	86.1	84	87	95	96	70	58	97	98	82	83	95	88	87	83	71	71	97	98
Ours	89.1	88.5	85	91	96	97	82	61	95	99	85	87	96	95	93	84	72	75	99	99

Place Dual Shoes		Pick Dual Bottles		Stack Bowls Three		Place A2B Left		Place A2B Right		Place Empty Cup		Move Can Pot		Place Cont. Plate		Press Stapler		Place Phone Stand		Place Fan	
C	R	C	R	C	R	C	R	C	R	C	R	C	R	C	R	C	R	C	R	C	R
75	75	93	63	77	71	87	82	87	84	100	99	51	55	99	95	87	83	81	81	87	85
90	89	88	85	72	76	76	80	77	70	100	100	75	66	96	98	90	95	84	96	94	89
75	87	93	88	75	82	79	77	76	76	100	99	82	90	95	96	92	94	91	91	93	86
91	93	87	88	83	76	80	83	81	79	100	100	75	75	100	98	92	95	91	96	97	91

Rotate QRcode		Place Obj. Stand		Shake Bottle		Scan Obj.		Pick Diverse Bottles		Place Bread Skillet		Place Bread Basket		Place Burger Fries		Place Cans Plasticbox		Put Bottles Dustbin		Hanging Mug	
C	R	C	R	C	R	C	R	C	R	C	R	C	R	C	R	C	R	C	R	C	R
89	87	91	85	99	97	18	17	81	71	85	66	77	64	94	87	94	84	84	79	77	71
78	86	96	90	100	99	57	47	78	69	91	91	90	90	96	96	98	98	80	83	72	76
83	87	96	85	98	99	56	38	80	74	89	91	91	91	95	99	99	96	88	87	75	82
88	87	98	96	100	100	49	57	83	80	89	87	92	91	99	97	99	99	94	93	83	76

4 Experiments

4.1 Setup

Testbeds. We evaluate EvoScene-VLA on two testbeds: the RoboTwin simulated benchmark [25] and the Galaxea R1-Lite real-robot platform. In simulation, our main evaluation uses 31 tasks; for ablations, we use a 5-task subset (*RoboTwin-5Task*) that spans single-arm, dual-arm, short-horizon, and long-horizon task types while keeping the ablation budget tractable, with the exact task list provided in Appendix D. We test two simulation settings. *Clean* fixes initial object positions to the training distribution. *Rand* randomizes initial positions and orientations within the task workspace. This randomization keeps the task goal unchanged but increases pose and layout variation.

Baselines. We fine-tune EvoScene-VLA from the public LingBot-VLA [40] pretrained checkpoint with the same 50-step action chunk. We compare against three baselines: $\pi_{0.5}$ [1], LingBot-VLA, and LingBot-VLA*. LingBot-VLA* adds depth supervision to LingBot-VLA.

4.2 Main Results

Tab. 1 reports per-task and average success rates on the 31 RoboTwin tasks. EvoScene-VLA improves the LingBot-VLA* average from 87.2 to 89.1 under *Clean* (+1.9) and from 86.1 to 88.5 under *Rand* (+2.4). The gain is larger under *Rand* (+2.4) than under *Clean* (+1.9). Two factors in *Rand* plausibly contribute: varied initial layouts make the scene harder to perceive from a single observation, and the resulting per-chunk perception errors are more likely to compound across chunks. The recurrent scene prefix is designed to mitigate both issues.

Fig. 1 examines the failure mode at the rollout level. For each of three tasks, the figure shows the LingBot-VLA* rollout next to ours from the same initial scene at three time slices (start, middle, end). Because chunked baselines plan the entire chunk from the start-state observation, they lack any view of the intermediate state that the chunk itself produces: in *Open Microwave*, the gripper retracts before reaching the door handle. EvoScene-VLA, whose action expert co-denoises a scene update alongside the action chunk, conditions on this intermediate scene state and continues the motion through to completion. The benefit also shows in motion quality. Fig. 3 plots end-effector trajectories in 3D for four episodes; EvoScene-VLA produces noticeably smoother paths than LingBot-VLA.

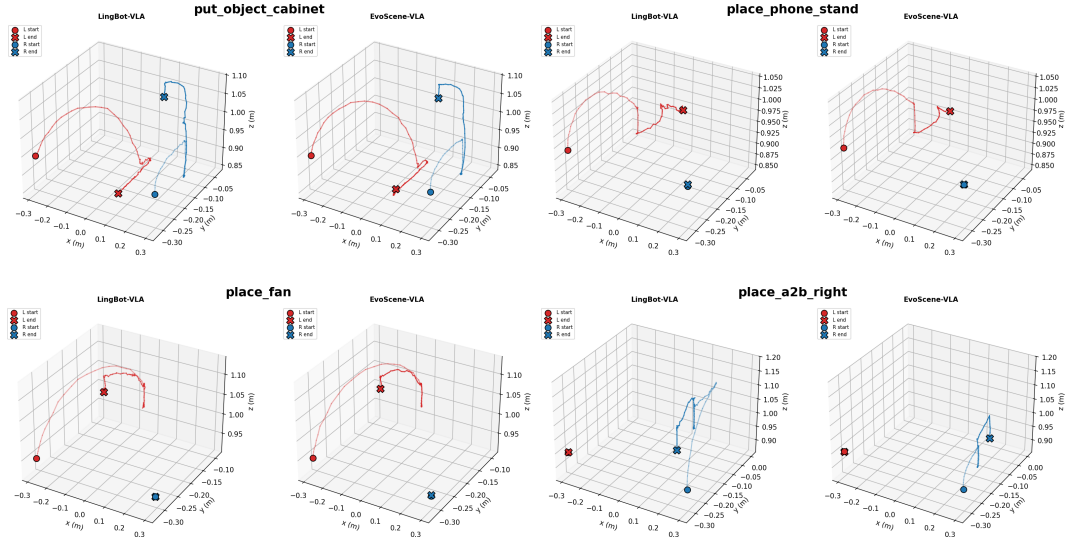


Figure 3: Trajectory plots in 3D space.

Table 2: **Ablations study.** Success rates averaged over the RoboTwin-5Task subset.

Variant	Clean	Rand
LingBot-VLA*	87.8	84.6
baseline	81.6	75.8
+ $\mathcal{L}_{\text{pred}}$ & \mathcal{L}_{rep}	89.3	86.2
+ \mathcal{L}_{geo}	90.1	86.5
+ prior info at inference	90.8	87.8

Table 3: **Real-robot experiments.** Success rates (%) on Galaxea indoor-cleaning tasks.

Task	$\pi_{0.5}$	LingBot VLA	LingBot VLA*	Ours
Mirror	28	27	26	29
Sink	42	44	49	51
Cutting-board	44	34	37	46
Avg. \uparrow(%)	38.0	35.0	37.3	42.0

Co-denosing ties each predicted action to a consistent scene context, so the action expert avoids the abrupt corrections of action-only chunked baselines.

4.3 Ablations

Tab. 2 reports additive ablations on RoboTwin-5Task. The first two rows show the LingBot-VLA and LingBot-VLA* baselines. Both lack our Geometric Anchor, Scene Predictor, and recurrent prior. The first step adds the global anchor (\mathcal{L}_{rep}) and Scene Predictor ($\mathcal{L}_{\text{pred}}$) jointly, since the two share the view-conditioned decoder and only become useful together. The local depth anchor (\mathcal{L}_{geo}) further improves performance by grounding each observation slot in per-view geometry, complementing the cross-view supervision from the global anchor. Finally, propagating the recurrent prior across chunks at inference, rather than reinitializing \bar{s}_t from learnable embeddings at every chunk, further improves performance and isolates the contribution of cross-chunk recurrence.

4.4 Real-Robot Evaluation

Platform and dataset. We evaluate EvoScene-VLA on the Galaxea R1-Lite dual-arm platform, training on the indoor-cleaning subset of the Galaxea Open-World Dataset [12] (mirror, sink, and cutting-board cleaning). Following the standard VLA interface, the policy uses one head stream and two wrist streams as its three-view input. The subset spans 7 recording sessions, 439 episodes, 48,419 frames, and 1,756 video clips, totaling approximately 9 hours of bimanual demonstrations at 15 fps. We use all demonstrations for training and evaluate on the physical robot.

Training and evaluation protocol. We initialize from the public LingBot-VLA checkpoint and fine-tune on the Galaxea indoor-cleaning subset with the same single-stage schedule. We evaluate on the Galaxea R1-Lite robot rather than replaying the dataset. We run all real-robot inference on a

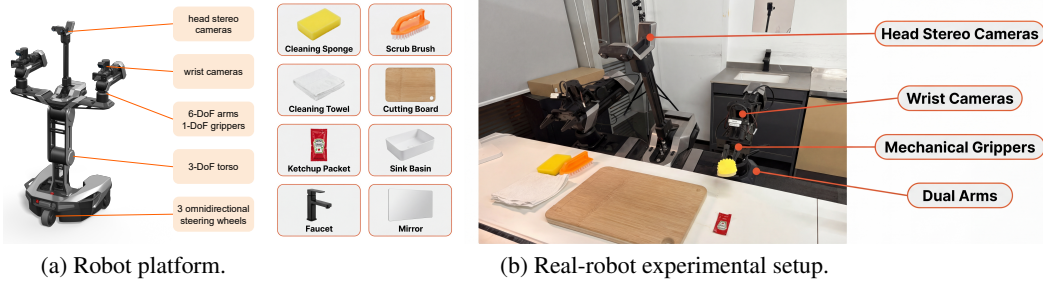


Figure 4: Real-robot platform and experimental setup. **(a)** The Galaxea R1-Lite platform uses three policy cameras for manipulation. **(b)** We evaluate the dual-arm robot on three cleaning tasks: *wiping the mirror*, *cleaning the sink*, and *cleaning the cutting board*. Ketchup serves as the removable stain.

single NVIDIA RTX 4090 GPU. The three long-horizon tasks (Wipe The Mirror, Clean The Sink, Clean The Cutting Board) require the robot to track how its tool changes the surface: the surface state evolves during wiping, and subsequent controls must target unwiped regions that can be subtle, occluded, or ambiguous in the current view. For each task, we run 100 closed-loop rollouts with randomized object placements, lighting, and initial robot state, and report task success rate.

Real-robot Results. Tab. 3 reports success rates on the Galaxea cleaning tasks. EvoScene-VLA improves average success from 37.3% to 42.0%. These gains show the same pattern as simulation: the method helps when the robot changes the scene as it acts.

5 Discussion

The experiments suggest a specific failure mode in chunked VLA control: the policy does not only need better current-frame geometry or longer observation history; it needs a prior for the scene after its own actions have changed it. EvoScene-VLA improves most in settings where this mismatch should matter, including randomized RoboTwin evaluation and real cleaning tasks with evolving surface state. This pattern supports the central design choice: the action decoder is a natural place to update scene state because it already generates the action sequence that will reshape the scene. The resulting prior does not need to be a dense reconstruction. A compact policy-facing latent can help if training grounds it in 3D structure and the next VLM call corrects it with fresh observations.

This view also clarifies the limits of the method. Because the recurrent state is latent, we judge its geometric content through downstream behavior and ablations. Because future scene targets come from future-frame 3D foundation-model features through Scene Predictor, target quality can limit the prior that the action decoder learns. Longer chunks may increase the value of recurrence by creating larger scene changes, but they also push Scene Predictor targets farther into the future, so the net effect of chunk length on prior quality remains an open question. A useful next step is to use the mismatch between observation slots and prior slots as an uncertainty signal for replanning or adaptive chunk execution. More broadly, the results suggest that action decoders can carry not only motor commands but also task-relevant scene priors, without adding an online world model at deployment.

6 Conclusion

EvoScene-VLA gives a chunked VLA a recurrent latent scene interface. The VLM prefix carries two slot groups. Observation slots read the current image. Prior slots inherit the evolved scene representation from the previous chunk. The action decoder jointly denoises motor commands and scene tokens at different key frames in one flow-matching pass. The scene token at the executed step becomes the next chunk’s prior. Training uses two-level Geometric Anchor and a training-only Scene Predictor to supply geometric and latent supervision; inference retains only the recurrent scene prefix and the action–scene co-denoising. On 31 RoboTwin tasks, EvoScene-VLA lifts average success from 87.2 to 89.1 under clean evaluation and from 86.1 to 88.5 under randomized initial conditions. Real-robot cleaning trials on Galaxea R1-Lite show the same pattern: the robot’s own actions evolve the scene state. For chunked VLAs, the action decoder should take the latent prior into account for the next visual update, rather than rebuilding it from each observation alone.

References

- [1] Kevin Black, Noah Brown, Danny Driess, Adnan Esmail, Michael Equi, Chelsea Finn, Niccolo Fusai, et al. π_0 : A vision-language-action flow model for general robot control. *arXiv preprint arXiv:2410.24164*, 2024.
- [2] Kevin Black, Mitsuhiko Nakamoto, Pranav Atreya, Homer Walke, Chelsea Finn, Aviral Kumar, and Sergey Levine. Zero-shot robotic manipulation with pretrained image-editing diffusion models. In *International Conference on Learning Representations (ICLR)*, 2024.
- [3] Anthony Brohan, Noah Brown, Justice Carbajal, Yevgen Chebotar, Xi Chen, Krzysztof Choromanski, et al. RT-2: Vision-language-action models transfer web knowledge to robotic control. In *Conference on Robot Learning (CoRL)*, 2023.
- [4] Chilam Cheang, Guangzeng Chen, Ya Jing, Tao Kong, Hang Li, Yifeng Li, Yuxiao Liu, Hongtao Wu, Jiafeng Xu, Yichu Yang, Hanbo Zhang, and Minzhao Zhu. GR-2: A generative video-language-action model with web-scale knowledge for robot manipulation. *arXiv preprint arXiv:2410.06158*, 2024.
- [5] Cheng Chi, Siyuan Feng, Yilun Du, Zhenjia Xu, Eric Cousineau, Benjamin Burchfiel, and Shuran Song. Diffusion policy: Visuomotor policy learning via action diffusion. In *Robotics: Science and Systems (RSS)*, 2023.
- [6] Nhat Chung, Taisei Hanyu, Toan Nguyen, Huy Le, Frederick Bumgarner, Duy Minh Ho Nguyen, Khoa Vo, Kashu Yamazaki, Chase Rainwater, Tung Kieu, Anh Nguyen, and Ngan Le. Rethinking progression of memory state in robotic manipulation: An object-centric perspective. *arXiv preprint arXiv:2511.11478*, 2025. Method named “Embodied-SlotSSM” inside the paper.
- [7] Yilun Du, Mengjiao Yang, Bo Dai, Hanjun Dai, Ofir Nachum, Joshua B. Tenenbaum, Dale Schuurmans, and Pieter Abbeel. Learning universal policies via text-guided video generation. In *International Conference on Machine Learning (ICML)*, 2023.
- [8] Ankit Goyal, Jie Xu, Yijie Guo, Valts Blukis, Yu-Wei Chao, and Dieter Fox. RVT: Robotic view transformer for 3d object manipulation. In *Conference on Robot Learning (CoRL)*, 2023.
- [9] Ankit Goyal, Valts Blukis, Jie Xu, Yijie Guo, Yu-Wei Chao, and Dieter Fox. RVT-2: Learning precise manipulation from few demonstrations. *arXiv preprint arXiv:2406.08545*, 2024.
- [10] Danijar Hafner, Jurgis Pasukonis, Jimmy Ba, and Timothy Lillicrap. Mastering diverse domains through world models. *arXiv preprint arXiv:2301.04104*, 2023.
- [11] Yucheng Hu, Yanjiang Guo, Pengchao Wang, Xiaoyu Chen, Yen-Jen Wang, Jianke Zhang, Koushil Sreenath, Chaochao Lu, and Jianyu Chen. Video prediction policy: A generalist robot policy with predictive visual representations. *arXiv preprint arXiv:2412.14803*, 2024.
- [12] Tao Jiang, Tianyuan Yuan, Yicheng Liu, Chenhao Lu, Jianning Cui, Xiao Liu, Shuiqi Cheng, Jiyang Gao, Huazhe Xu, and Hang Zhao. Galaxea open-world dataset and G0 dual-system VLA model. *arXiv preprint arXiv:2509.00576*, 2025. URL <https://arxiv.org/abs/2509.00576>. <https://github.com/OpenGalaxea/GalaxeaVLA>.
- [13] Moo Jin Kim, Karl Pertsch, Siddharth Karamcheti, Ted Xiao, Ashwin Balakrishna, Suraj Nair, et al. OpenVLA: An open-source vision-language-action model. *arXiv preprint arXiv:2406.09246*, 2024.
- [14] Po-Chen Ko, Jiayuan Mao, Yilun Du, Shao-Hua Sun, and Joshua B. Tenenbaum. Learning to act from actionless videos through dense correspondences. In *International Conference on Learning Representations (ICLR)*, 2024.
- [15] Myungkyu Koo, Daewon Choi, Taeyoung Kim, Kyungmin Lee, Changyeon Kim, Younggyo Seo, and Jinwoo Shin. HAMLET: Switch your vision-language-action model into a history-aware policy. *arXiv preprint arXiv:2510.00695*, 2025.
- [16] Vincent Leroy, Yohann Cabon, and Jerome Revaud. Grounding image matching in 3d with MAST3R. *arXiv preprint arXiv:2406.09756*, 2024.

- [17] Fuhao Li, Wenxuan Song, Han Zhao, Jingbo Wang, Pengxiang Ding, Donglin Wang, Long Zeng, and Haoang Li. Spatial forcing: Implicit spatial representation alignment for vision-language-action model. *arXiv preprint arXiv:2510.12276*, 2025.
- [18] Xiaoqi Li, Liang Heng, Jiaming Liu, Yan Shen, Chenyang Gu, Zhuoyang Liu, Hao Chen, Nuwei Han, Renrui Zhang, Hao Tang, Shanghang Zhang, and Hao Dong. 3DS-VLA: A 3d spatial-aware vision language action model for robust multi-task manipulation. In *Conference on Robot Learning (CoRL)*, 2025.
- [19] Yixuan Li, Yuhui Chen, Mingcai Zhou, Haoran Li, Zhengtao Zhang, and Dongbin Zhao. QDepth-VLA: Quantized depth prediction as auxiliary supervision for vision-language-action models. *arXiv preprint arXiv:2510.14836*, 2025.
- [20] Minghui Lin, Pengxiang Ding, Shu Wang, Zifeng Zhuang, Yang Liu, Xinyang Tong, Wenxuan Song, Shangke Lyu, Siteng Huang, and Donglin Wang. HiF-VLA: Hindsight, insight and foresight through motion representation for vision-language-action models. *arXiv preprint arXiv:2512.09928*, 2025.
- [21] Yaron Lipman, Ricky T. Q. Chen, Heli Ben-Hamu, Maximilian Nickel, and Matt Le. Flow matching for generative modeling. In *International Conference on Learning Representations (ICLR)*, 2023.
- [22] Songming Liu, Lingxuan Wu, Bangguo Li, Hengkai Tan, Huayu Chen, Zhengyi Wang, Ke Xu, Hang Su, and Jun Zhu. RDT-1B: A diffusion foundation model for bimanual manipulation. *arXiv preprint arXiv:2410.07864*, 2024.
- [23] Xingchao Liu, Chengyue Gong, and Qiang Liu. Flow straight and fast: Learning to generate and transfer data with rectified flow. In *International Conference on Learning Representations (ICLR)*, 2023.
- [24] Guanxing Lu, Shiyi Zhang, Ziwei Wang, Changliu Liu, Jiwen Lu, and Yansong Tang. Mani-Gaussian: Dynamic gaussian splatting for multi-task robotic manipulation. *arXiv preprint arXiv:2403.08321*, 2024.
- [25] Yao Mu, Tianxing Chen, Shijia Peng, Zanxin Chen, Zeyu Gao, Yude Zou, Lunkai Lin, Zhiqiang Xie, and Ping Luo. RoboTwin: Dual-arm robot benchmark with generative digital twins. *arXiv preprint arXiv:2409.02920*, 2024.
- [26] Octo Model Team, Dibya Ghosh, Homer Walke, Karl Pertsch, et al. Octo: An open-source generalist robot policy. *arXiv preprint arXiv:2405.12213*, 2024.
- [27] Aaditya Prasad, Kevin Lin, Jimmy Wu, Linqi Zhou, and Jeannette Bohg. Consistency policy: Accelerated visuomotor policies via consistency distillation. *arXiv preprint arXiv:2405.07503*, 2024.
- [28] Delin Qu et al. SpatialVLA: Exploring spatial representations for visual-language-action models. *arXiv preprint arXiv:2501.15830*, 2025.
- [29] Robbyant Team. LingBot-Depth: Masked depth modeling for spatial perception. <https://huggingface.co/robyant/lingbot-depth>, 2026. Open-source RGB-D representation model used as the frozen depth teacher.
- [30] Hao Shi, Bin Xie, Yingfei Liu, Lin Sun, Fengrong Liu, Tiancai Wang, Erjin Zhou, Haoqiang Fan, Xiangyu Zhang, and Gao Huang. MemoryVLA: Perceptual-cognitive memory in vision-language-action models for robotic manipulation. *arXiv preprint arXiv:2508.19236*, 2025.
- [31] Mohit Shridhar, Lucas Manuelli, and Dieter Fox. Perceiver-actor: A multi-task transformer for robotic manipulation. In *Conference on Robot Learning (CoRL)*, 2022.
- [32] Bin Tan, Changjiang Sun, Xiage Qin, Hanat Adai, Zelin Fu, Tianxiang Zhou, Han Zhang, Yinghao Xu, Xing Zhu, Yujun Shen, et al. Masked depth modeling for spatial perception. *arXiv preprint arXiv:2601.17895*, 2026.

- [33] Lirui Wang, Xinlei Chen, Jialiang Zhao, and Kaiming He. HPT: Scaling proprioceptive-visual learning with heterogeneous pre-trained transformers. *arXiv preprint arXiv:2409.20537*, 2024.
- [34] Qianqian Wang, Yifei Zhang, Aleksander Holynski, Alexei A. Efros, and Angjoo Kanazawa. Continuous 3D perception model with persistent state. *arXiv preprint arXiv:2501.12387*, 2025.
- [35] Shuzhe Wang, Vincent Leroy, Yohann Cabon, Boris Chidlovskii, and Jerome Revaud. DUS3R: Geometric 3D vision made easy. In *IEEE/CVF Conference on Computer Vision and Pattern Recognition (CVPR)*, 2024.
- [36] Yifan Wang, Jianjun Zhou, Haoyi Zhu, Wenzheng Chang, Yang Zhou, Zizun Li, Junyi Chen, Jiangmiao Pang, Chunhua Shen, and Tong He. π^3 : Permutation-equivariant visual geometry learning. In *International Conference on Learning Representations (ICLR)*, 2026.
- [37] Chuan Wen, Xingyu Lin, John So, Kai Chen, Qi Dou, Yang Gao, and Pieter Abbeel. Any-point trajectory modeling for policy learning. *arXiv preprint arXiv:2401.00025*, 2024.
- [38] Hongtao Wu, Ya Jing, Chilam Cheang, Guangzeng Chen, Jiafeng Xu, Xinghang Li, Minghuan Liu, Hang Li, and Tao Kong. Unleashing large-scale video generative pre-training for visual robot manipulation. *arXiv preprint arXiv:2312.13139*, 2023.
- [39] Philipp Wu, Alejandro Escontrela, Danijar Hafner, Pieter Abbeel, and Ken Goldberg. Day-Dreamer: World models for physical robot learning. In *Conference on Robot Learning (CoRL)*, 2022.
- [40] Wei Wu, Fan Lu, Yunnan Wang, Shuai Yang, Shi Liu, Fangjing Wang, Qian Zhu, He Sun, Yong Wang, Shuailei Ma, Yiyu Ren, Kejia Zhang, Hui Yu, Jingmei Zhao, Shuai Zhou, Zhenqi Qiu, Houlong Xiong, Ziyu Wang, Zechen Wang, Ran Cheng, Yong-Lu Li, Yongtao Huang, Xing Zhu, Yujun Shen, and Kecheng Zheng. LingBot-VLA: A pragmatic vla foundation model. *arXiv preprint arXiv:2601.18692*, 2026.
- [41] Lei Xiao, Jifeng Li, Juntao Gao, Feiyang Ye, Yan Jin, Jingjing Qian, Jing Zhang, Yong Wu, and Xiaoyuan Yu. AVA-VLA: Improving vision-language-action models with active visual attention. *arXiv preprint arXiv:2511.18960*, 2025.
- [42] Yanjie Ze, Gu Zhang, Kangning Zhang, Chenyuan Hu, Muhan Wang, and Huazhe Xu. 3D diffusion policy: Generalizable visuomotor policy learning via simple 3D representations. *arXiv preprint arXiv:2403.03954*, 2024.
- [43] Jianke Zhang, Yanjiang Guo, Yucheng Hu, Xiaoyu Chen, Xiang Zhu, and Jianyu Chen. UP-VLA: A unified understanding and prediction model for embodied agent. *arXiv preprint arXiv:2501.18867*, 2025.
- [44] Ruijie Zheng, Yongyuan Liang, Shuaiyi Huang, Jianfeng Gao, Hal Daumé III, Andrey Kolobov, Furong Huang, and Jianwei Yang. TraceVLA: Visual trace prompting for generalist robot policies. *arXiv preprint arXiv:2412.10345*, 2024.
- [45] Ruijie Zheng, Jing Wang, Scott Reed, Johan Bjorck, Yu Fang, Fengyuan Hu, Joel Jang, Kaushil Kundalia, Zongyu Lin, Loic Magne, Avnish Narayan, You Liang Tan, Guanzhi Wang, Qi Wang, Jiannan Xiang, Yinzhen Xu, Seonghyeon Ye, Jan Kautz, Furong Huang, Yuke Zhu, and Linxi Fan. FLARE: Robot learning with implicit world modeling. *arXiv preprint arXiv:2505.15659*, 2025.
- [46] Hanyu Zhou, Chuanhao Ma, and Gim Hee Lee. VLA-4D: Embedding 4d awareness into vision-language-action models for spatiotemporally coherent robotic manipulation. *arXiv preprint arXiv:2511.17199*, 2025.

Overview

This appendix supplements the main paper with implementation, evaluation, and discussion details. Appendix A reports the optimization recipe, hyperparameters (Tab. 4), and frozen-teacher pipeline. Appendix B (Tab. 5) consolidates the symbols used throughout the method, and Appendix C provides pseudocode for one training step (Algorithm 1) and one inference chunk (Algorithm 2). Appendix D lists the 31 RoboTwin tasks, the RoboTwin-5Task ablation subset, and baseline configurations, while Appendix E presents additional 3D end-effector trajectory comparisons (Fig. 5). We close with limitations (Appendix F) and broader impact (Appendix G).

A Implementation

Optimisation recipe. Following LingBot-VLA’s recipe (Tab. 4), the action expert is held in fp32 while the rest of the model runs in bf16 storage with fp32 reductions. The full model optimizes Eq. (12); the w/o Geometric Anchor variant drops the local and global anchor losses.

Hyperparameters. The loss weights λ_1 – λ_4 in Tab. 4 are tuned on RoboTwin-5Task and reused on the full RoboTwin and Galaxea evaluations without further sweeping.

Table 4: Hyperparameters introduced by EvoScene-VLA. Optimisation values are inherited from the LingBot-VLA recipe; loss weights are EvoScene-VLA-specific.

Optimisation	
Optimiser	AdamW
Learning rate (constant)	1×10^{-4}
Effective batch size	256
Total update steps	20,000
Mixed precision	bf16 storage / fp32 reductions
Hardware	8×A800
Architecture	
VLM backbone	Qwen2.5-VL-3B-Instruct
Hidden dimension D	2048
Camera views V	3 (head, left wrist, right wrist)
Image resolution	224×224
Template bank size	256
Observation / prior slots N	16
Key frames K	3
Action chunk length	50
Loss weights (Eq. (12))	
λ_1 on \mathcal{L}_{geo}	0.04
λ_2 on \mathcal{L}_{rep}	0.10
λ_3 on $\mathcal{L}_{\text{pred}}$	0.10
λ_4 on $\mathcal{L}_{\text{sceneFM}}$	0.01
Inference	
Flow-matching Euler steps	10
Re-observation period	1 chunk (50 steps)

Frozen teachers. The local depth head g_{depth} reuses the LingBot-Depth alignment block, supervised by LingBot-VLA’s MoRGBD pipeline [32] (MoGe-2 ViT-B normal variant combined with the LingBot-Depth masked-depth-modeling teacher) on the unmasked target view. The global 3D supervisor is the frozen Pi³ multi-view 3D foundation model [36], applied to the current-frame multi-view input for \mathcal{L}_{rep} and to the future-frame multi-view input for $\mathcal{L}_{\text{pred}}$.

B Notation

Tab. 5 consolidates the symbols used throughout Secs. 3.2 to 3.5.

Table 5: Notation used in EvoScene-VLA. Shapes are written as $\mathbb{R}^{(\text{dimensions})}$ where applicable.

Symbol	Meaning
<i>Indices and dimensions</i>	
t	Discrete time index of the current control chunk
D	VLM hidden dimension (Qwen2.5-VL-3B: $D=2048$)
V	Number of camera views ($V=3$: head, left wrist, right wrist)
N	Number of slots per observation or prior group ($N=16$)
K	Number of scene key-frame query groups ($K=3$)
H	Final action offset of the chunk; chunk length $H+1=50$
$\{k_1, \dots, k_K\}$	Sparse key-frame offsets, $k_i \in \{1, \dots, H\}$
<i>Inputs</i>	
x_t	Multi-view image input at step t
x_{t,v_i}	Image of view $i \in \{1, \dots, V\}$
ℓ	Language instruction
r_t	Robot proprioceptive state
$a_{t:t+H}$	Ground-truth action chunk
<i>Recurrent scene prefix</i>	
$s_{\text{obs}}^{(v)} \in \mathbb{R}^{N \times D}$	Observation slots for view v , gather geometric evidence per camera
$\bar{s}_t \in \mathbb{R}^{N \times D}$	Prior slots inherited from the previous chunk
$s_p \in \mathbb{R}^{N \times D}$	VLM output at the prior-slot positions; cross-view scene representation
$h_{t,v}^{\text{img}}$	VLM image tokens for view v
$m \in \mathbb{R}^D$	Learned mask embedding for cross-view masking
<i>Geometric Anchor (training only)</i>	
q_{templ}	256-token template query bank reused for g_{depth}
g_{depth}	Cross-attention head producing per-view depth representations
$\hat{f}_{t,i}^d$	Predicted depth representation for masked target view i
MDT	Frozen Monocular Depth Teacher (MoGe-2 + LingBot-Depth)
g_{3D}	View-conditioned cross-attention decoder for the global anchor
q_{dec}	Learnable view-aware queries for g_{3D}
W_{proj}	Linear projector to the 3D foundation-model feature space
P_t, Z_t	Projected output / frozen 3DFM features for the current frame
<i>Scene Predictor (training only)</i>	
q_1, \dots, q_K	Key-frame query groups initialized from s_p , each of size N
$\hat{s}_{t+k_i} \in \mathbb{R}^{N \times D}$	Predicted absolute future scene latent at offset k_i
$\tilde{P}_{t+k_i}, Z_{t+k_i}$	Projected predicted feature / frozen 3DFM feature on the future frame
<i>Joint action–scene flow matching</i>	
$z_0 \in \mathbb{R}^{K \times N \times D}$	Standardised future-scene targets (LayerNorm of \hat{s})
$\tau \in [0, 1]$	Shared flow-matching time
ϵ_a, ϵ_s	Independent Gaussian noises on action / scene paths
$a_{t:t+H}^\tau, z^\tau$	Straight-line interpolants
$v_\theta^{(a)}, v_\theta^{(s)}$	Predicted velocities for action / scene blocks
<i>Losses (Eq. (12))</i>	
\mathcal{L}_{geo}	Cross-view masked depth reconstruction loss
\mathcal{L}_{rep}	Global anchor ℓ_1 loss for the current frame
$\mathcal{L}_{\text{pred}}$	Future-scene ℓ_1 loss for the K key frames
$\mathcal{L}_{\text{sceneFM}}$	Scene flow-matching loss in the action expert
$\mathcal{L}_{\text{actFM}}$	Action flow-matching loss in the action expert
$\lambda_1, \lambda_2, \lambda_3, \lambda_4$	Loss weights (0.04, 0.10, 0.10, 0.01)

C Algorithms

Algorithm 1 states one training step. Algorithm 2 states the deployed forward path.

Algorithm 1 EvoScene-VLA training step.

Require: Sample $(x_t, \ell, r_t, a_{t:t+H}, x_{t+k_1}, \dots, x_{t+k_K})$ and prior carry \bar{s}_t (learnable embedding for the first chunk in an episode).

- 1: Form prefix $[x_t, s_{\text{obs}}^{(1:V)}, \bar{s}_t, \ell]$ with the asymmetric attention mask (Sec. 3.2).
- 2: Run VLM forward; read s_p from the prior-slot positions (Eq. (2)).
- 3: **for** each view $i \in \{1, \dots, V\}$ **do** ▷ Local depth anchor
- 4: Mask $h_{t,v_i}^{\text{img}} \leftarrow m$, keep other views unchanged.
- 5: $\hat{f}_{t,i}^d \leftarrow g_{\text{depth}}(q_{\text{tmpl}}, [\tilde{h}_{t,v_1:V}^{\text{img},(i)}, s_p])$
- 6: **end for**
- 7: $\mathcal{L}_{\text{geo}} \leftarrow \frac{1}{V} \sum_i \text{SmoothL1}(\hat{f}_{t,i}^d, \text{MDT}(x_{t,v_i}))$ ▷ Eq. (4)
- 8: $P_t \leftarrow W_{\text{proj}} g_{3\text{D}}(q_{\text{dec}}; s_p)$ ▷ Global anchor
- 9: $\mathcal{L}_{\text{rep}} \leftarrow \frac{1}{V} \sum_v \|P_t^{(v)} - 3\text{DFM}(x_t)^{(v)}\|_1$
- 10: $\hat{s}_{t+k_1:t+k_K} \leftarrow \text{ScenePredictor}(r_t, s_p, a_{t:t+H}, q_1, \dots, q_K)$
- 11: $\tilde{P}_{t+k_i} \leftarrow W_{\text{proj}} g_{3\text{D}}(q_{\text{dec}}; \hat{s}_{t+k_i})$ **for each** i
- 12: $\mathcal{L}_{\text{pred}} \leftarrow \frac{1}{KV} \sum_{i,v} \|\tilde{P}_{t+k_i}^{(v)} - 3\text{DFM}(x_{t+k_i})^{(v)}\|_1$
- 13: $z_0 \leftarrow \text{LayerNorm}(\hat{s}_{t+k_1:t+k_K})$ ▷ Standardise future-scene targets
- 14: **Sample** $\tau \sim \mathcal{U}[0, 1], \epsilon_a, \epsilon_s \sim \mathcal{N}(0, I)$
- 15: $a^\tau \leftarrow \tau \epsilon_a + (1-\tau)a_{t:t+H}, z^\tau \leftarrow \tau \epsilon_s + (1-\tau)z_0$
- 16: $v_\theta^{(a)}, v_\theta^{(s)} \leftarrow \text{ActionExpert}([r_t | z^\tau | a^\tau]; \text{prefix cache})$
- 17: $\mathcal{L}_{\text{actFM}} \leftarrow \|v_\theta^{(a)} - (\epsilon_a - a_{t:t+H})\|_2^2$
- 18: $\mathcal{L}_{\text{sceneFM}} \leftarrow \|v_\theta^{(s)} - (\epsilon_s - z_0)\|_2^2$
- 19: $\mathcal{L} \leftarrow \mathcal{L}_{\text{actFM}} + \lambda_1 \mathcal{L}_{\text{geo}} + \lambda_2 \mathcal{L}_{\text{rep}} + \lambda_3 \mathcal{L}_{\text{pred}} + \lambda_4 \mathcal{L}_{\text{sceneFM}}$
- 20: Backpropagate \mathcal{L} ; update VLM, action expert, and all training-only modules.

Algorithm 2 EvoScene-VLA inference per chunk.

Require: Current observation x_t , instruction ℓ , robot state r_t , prior buffer \bar{s}_t (learnable embedding for the first chunk).

Ensure: Action chunk $\hat{a}_{t:t+H}$ executed on the robot; updated prior \bar{s}_{t+1} .

- 1: Form prefix $[x_t, s_{\text{obs}}^{(1:V)}, \bar{s}_t, \ell]$ and run one VLM forward.
- 2: Read s_p at the prior-slot positions; cache the prefix KV. ▷ Geometric Anchor / Scene Predictor not loaded.
- 3: Initialise $a^1 \sim \mathcal{N}(0, I), z^1 \sim \mathcal{N}(0, I)$.
- 4: **for** each Euler step $\tau \in \{1, 1-\Delta\tau, \dots, \Delta\tau\}$ (10 steps total) **do**
- 5: $v^{(a)}, v^{(s)} \leftarrow \text{ActionExpert}([r_t | z^\tau | a^\tau]; \text{prefix cache})$
- 6: $a^{\tau-\Delta\tau} \leftarrow a^\tau - \Delta\tau v^{(a)}, z^{\tau-\Delta\tau} \leftarrow z^\tau - \Delta\tau v^{(s)}$
- 7: **end for**
- 8: $\hat{a}_{t:t+H} \leftarrow a^0; \hat{s}_{t+k_1:t+k_K} \leftarrow z^0$ ▷ Joint denoised outputs
- 9: **Execute** $\hat{a}_{t:t+H}$ on the robot.
- 10: $\bar{s}_{t+1} \leftarrow \hat{s}_{t+k_K}$ ▷ Write the executed end-point token back as the next prior
- 11: **Re-observe** x_{t+1} and return to step 1 for the next chunk.

D Datasets and Tasks

RoboTwin 31 tasks. We use 31 language-conditioned manipulation tasks from RoboTwin 2.0 [25], covering single-arm and dual-arm, short-horizon and long-horizon settings. The full task list is: place_mouse_pad, click_bell, open_microwave, place_shoe, put_object_cabinet, stack_blocks_three, beat_block_hammer, turn_switch, open_laptop, place_dual_shoes, pick_dual_bottles, stack_bowls_three, place_a2b_left, place_a2b_right, place_empty_cup, move_can_pot, place_container_plate, press_stapler, place_phone_stand, place_fan, rotate_qrcode, place_object_stand, shake_bottle, scan_object, pick_diverse_bottles, place_bread_skillet, place_bread_basket, place_burger_fries, place_cans_plasticbox,

put_bottles_dustbin, and hanging_mug. Each task uses RoboTwin’s standard episode length and the 50-step action chunk.

RoboTwin-5Task ablation subset. For ablations we use a 5-task subset that spans single-arm, dual-arm, short-horizon, and long-horizon types and keeps the ablation budget controlled: click_bell, open_microwave, place_shoe, put_object_cabinet, and stack_blocks_three.

Baselines. LingBot-VLA* is the depth-augmented LingBot-VLA, corresponding to the robotwin_load20000h_depth configuration of the LingBot-VLA repository. EvoScene-VLA shares its training data, chunk length, and compute budget with all baselines.

E Additional Trajectory Visualizations

Fig. 5 shows additional 3D end-effector trajectory comparisons complementing Fig. 3.

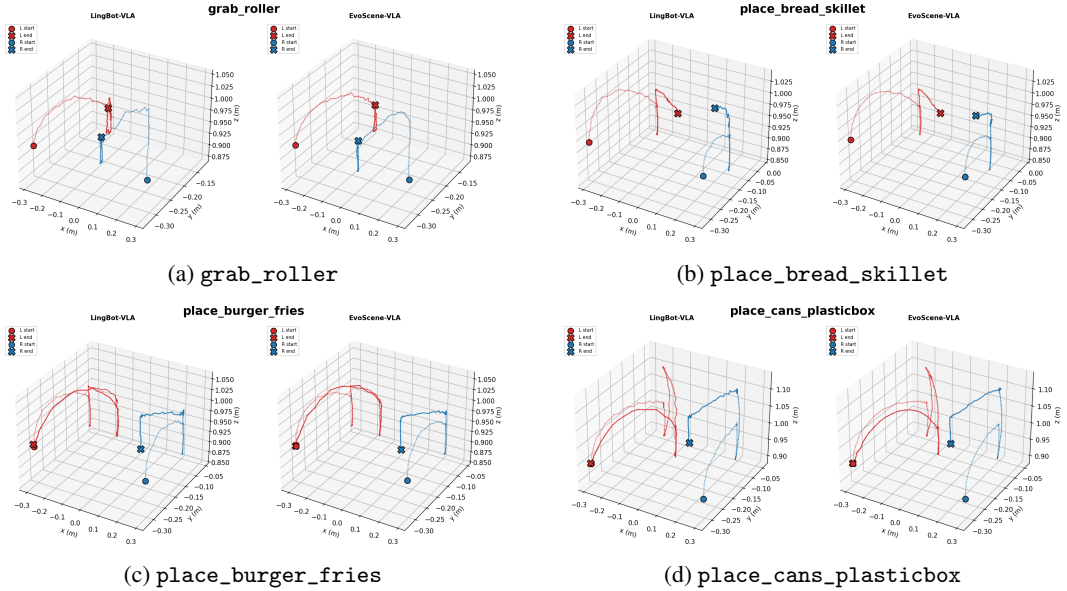


Figure 5: Additional 3D end-effector trajectory comparisons on four RoboTwin tasks, complementing Fig. 3. EvoScene-VLA produces noticeably smoother paths than LingBot-VLA across all four cases.

F Limitations

EvoScene-VLA carries a latent recurrent state across chunk boundaries, so its geometric content is not directly interpretable; the value of the prior must be judged through downstream behavior and through the controlled ablation in Tab. 2. Future-scene supervision flows through a frozen 3D foundation model on future frames, so target quality upper-bounds the prior the action expert can learn. We train Scene Predictor and the action expert’s scene branch only at a fixed set of key-frame offsets $\{k_1, \dots, k_K\}$. Deployments that re-observe at intervals diverging from these offsets therefore receive a temporally misaligned prior at the next chunk. Real-robot evaluation is currently limited to three indoor-cleaning tasks on a single dual-arm platform; behavior under category shift, novel scenes, and multi-step task chaining remains future work.

G Broader Impact

EvoScene-VLA is a manipulation policy aimed at indoor household assistance. Robots that run such policies inside homes raise standard considerations around physical safety, user privacy from on-robot camera streams, and potential displacement of routine paid labor. These considerations apply to vision–language–action policies broadly and are not specific to the recurrent scene prefix introduced

here. All training data in this work come from public datasets or platform-provided demonstrations under their respective licences; real-robot evaluation is conducted in a controlled lab setting with no human subjects.